

DESIGN AND OPERATION OF GRID CONNECTED PV SYSTEM BASED ON HIGH PERFORMANCE CONSTANT POWER GENERATION BY USING ANN CONTROLLER

¹D.ARAVIND, ²V.SUNIL KUMAR, ³ISMAYEL GOLLAPUDI,

¹Assistant Professor, St. Martin’s Engineering College, Dhullapally, Secunderabad, Telangana.

²Associate Professor St. Martin’s Engineering College, Dhullapally, Secunderabad, Telangana.

³Assistant Professor, MallaReddy Engineering College and Management science

ABSTRACT: In this paper an improved control strategy is implemented the incremental method of the maximum power which is feed to the PV systems with ANN control and it is proposed to make sure about the smooth and fast transition between Constant Power Generation (CPG) and maximum power point tracking and also by the proposed control strategy we can always achieved the stable operation. ANN is nonlinear model that is easy to use and understand compared to statistical methods. ANN is non-paramateric model while most of statistical methods are parametric model that need higher background of statistic. Regardless of the solar irradiance levels and high-performance. Which can be regulate by the PV output power according to any set-point, and it also force the PV systems to operate at the left side of the maximum power point without any stability problems. Here we are using the ANN controller compared to other controllers the efficiency of the system improves. Simulation results have been verified in the effectiveness manner by using the proposed CPG control in terms of high accuracy, stable transitions, and fast dynamics.

Index Terms—Active power control, constant power control, maximum power point tracking, PV systems, power converters, ANN control.

INTRODUCTION

In the recent year, Maximum Power Point Tracking (MPPT) operation is necessary in the grid-connected PV systems in order to get the maximize power from the energy yield. PV installations is need for the advance power control schemes and along with the regulations to decrease impacts from PV systems such as the overloading the power grid. For the German Federal Law: Renewable Energy Sources Act in which the PV systems with the rated power below 30 kWp which have the limit for the maximum which is feed to the power (e.g. 70 % of the rated power) which can be remotely controlled by the utility like the active power control which is referred as the Constant Power Generation (CPG) control or an absolute power control which is described in the Danish grid code in which CPG

concept which have been presented which is reveals by the most cost-effective way to achieve the CPG control is by modifying the MPPT algorithm at the PV inverter level. Specifically, the PV system is operated in the MPPT mode, when the PV output power P_{pv} is below the setting-point P_{limit} .

$$P_{PV} = \begin{cases} P_{MPPT}, & \text{when } P_{PV} \leq P_{limit} \\ P_{limit}, & \text{when } P_{PV} > P_{limit} \end{cases} \quad (1)$$

Moreover, whenever the output power reach the Limit, then the output power of the PV system will be kept constant, i.e., $P_{PV} = P_{limit}$ which leading to the constant active power which is injected as shown in (1) and it also illustrated in Fig. 1 In terms of the algorithms and the CPG which is based upon the Perturb and Observe (P&O-CPG) algorithm which was introduced by the single stage PV systems. moreover during the operating area of the CPG control which is limited at the right side of the Maximum Power Point (MPP) of the PV arrays (CPP-R), due to its single-stage configuration. Unfortunately it will reduce the robustness of the control algorithm when the PV systems is experience with the fast decrease during the irradiance time.

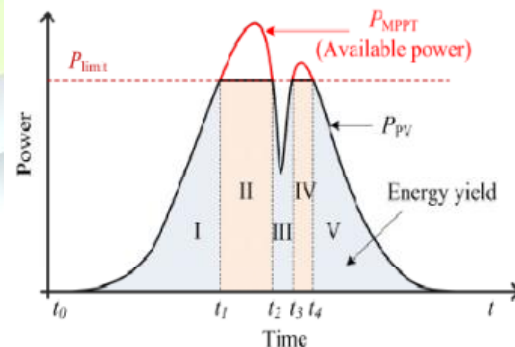


Fig. 1. Constant Power Generation (CPG) concept: 1) MPPT mode during I, III, V, and 2) CPG mode during II, IV [6].

The operating point may go through the open-circuit condition which is illustrated and shown in the Fig. 2. A two-stage grid-connected PV is implemented to extend the operating area of the

P&O-CPG algorithm. And also by regulating the PV output power which at the left side of the MPP (CPP-L) as shown in Fig. 2, where the stable CPG operation is always achieved by the operating point which will never “fall off the hill” during a fast reduce in the irradiance.

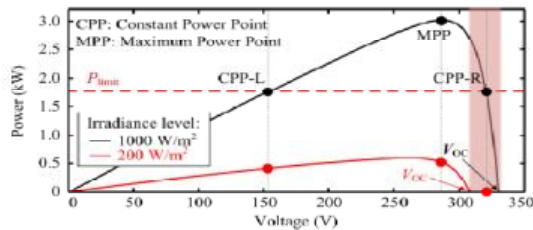


Fig. 2. Stability issues of the conventional CPG algorithms, when the operating point is normally located at the right side of the MPP..

CONVENTIONAL CPG ALGORITHM

System Configuration

As shown in the Fig. 3 shows the basic hardware configuration of the two-stage single-phase grid-connected PV system and its control structure. The CPG control is developed in the boost converter, which have been explained in the next section.

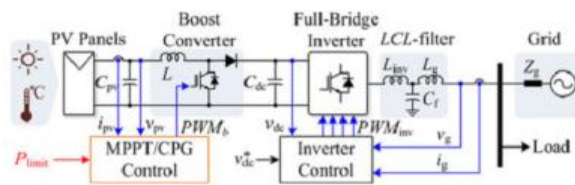


Fig. 3. Simulation of schematic and overall control structure of a two-stage single phase grid-connected PV system

The full-bridge inverter control is realized by the cascaded control, here the DC-link voltage is kept constant throughout the control of the AC grid current, which is an inner loop an active power is injected to the grid, which meaning that the PV system operates at a unity power factor. Not only that have been mentioned above and the two-stage configuration can extend the operating range of both the MPPT and CPG algorithms. In the two-stage case, the PV output voltage v_{pv} can be lower (e.g., at the left side of the MPP), and then it can be stepped up by the boost converter to match the required DC-link voltage (e.g., 450 V). This is not the case for the single-stage configuration, where the PV output voltage v_{pv} is directly fed to the PV inverter and has to be higher than the grid voltage level (e.g., 325 V) to ensure the power delivery. Christo Ananth et al.[4] presented a brief outline on Electronic Devices and

Circuits which forms the basis of the Clampers and Diodes.

Operational Principle

The operational principle of the conventional P&O-CPG algorithm is illustrated in Fig. 4. It can be divided into two modes: a) MPPT mode ($P_{pv} < P_{limit}$), where the P&O algorithm should track the maximum power; b) CPG mode ($P_{pv} > P_{limit}$), where the PV output power is limited at P_{limit} . During the MPPT operation, the behavior of the algorithm is similar to the conventional P&O MPPT algorithm - the operating point will track and oscillate around the MPP.

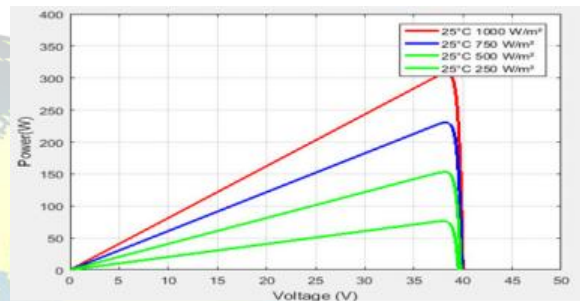


Fig. 4. Operational principle of the Perturb and Observe based CPG algorithm (P&O-CPG), where the operating point is regulated to the left side of the MPP considering stability issues.

In the case of the CPG operation, the PV voltage v_{pv} is continuously perturbed toward a point referred to as Constant Power Point (CPP), i.e., $P_{pv} = P_{limit}$. After a number of iterations, the operating point will reach and oscillate around the CPP. Although the PV system with the P&O-CPG control can operate at both CPPs, only the operation at the left side of the MPP (CPP-L) is focused for the stability concern. The control structure of the algorithm is shown in Fig. 5, where v^*_{pv} can be expressed as

$$v^*_{pv} = \begin{cases} v_{MPPT}, & \text{when } P_{pv} \leq P_{limit} \\ v_{pv,n} - v_{step}, & \text{when } P_{pv} > P_{limit} \end{cases} \quad (2)$$

where v_{MPPT} is the reference voltage from the MPPT algorithm (i.e., the P&O MPPT algorithm), $v_{pv,n}$ is the measured PV voltage, and v_{step} is the perturbation step size.

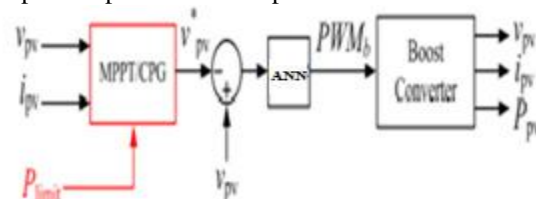


Fig. 5. Control structure of the Perturb and Observe based CPG algorithm (P&O-CPG), where a Proportional Integrator (PI) is adopted.

Issues Of The P&O-CPG Algorithm

The P&O-CPG algorithm has a satisfied performance under slow changing irradiance conditions, e.g., during a clear day, when the operating point is at the left side of the MPP, as shown in Fig. 6(a). However, irradiance fluctuation that may happen in a cloudy day will result in overshoots and power losses as shown in Fig. 6(b).

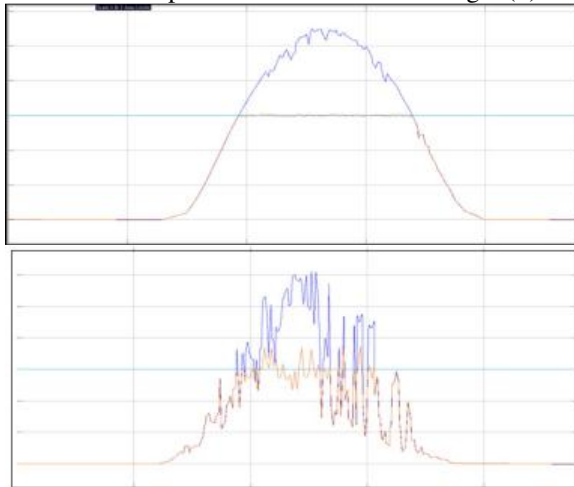


Fig. 6. simulation results of the Perturb and Observe based CPG algorithm (P&O-CPG) under two daily conditions: (a) clear day and (b) cloudy day.

This can be further explained using the operation trajectory of the PV system presented in Fig6. Assuming that the PV system is operating in MPPT mode initially and the irradiance level suddenly increases, the PV power P_{pv} is basically lifted by the change in the irradiance, as it can be seen from the black arrow trajectory (i.e., A!B!C). As a consequence, large power overshoots may occur. Similarly, if the PV system is operating in the CPG operation (e.g., at CPP-L) and the irradiance suddenly drops, the output power P_{pv} will make a sudden decrease, as shown in Fig. (i.e., CID). It will take a number of iterations until the operating point reaches the new MPP (i.e., E) at that irradiance condition (i.e., 200 W/m²), and resulting in loss of power generation.

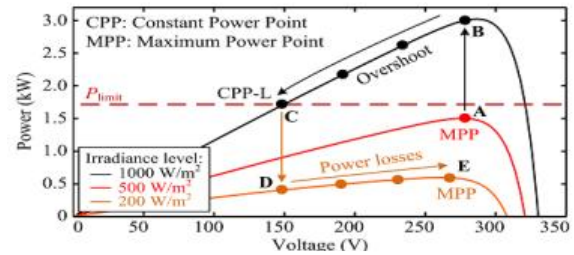


Fig. 7. Operating trajectory of the algorithm during a fast changing irradiance condition resulting in overshoot (black arrow) and power losses (orange arrow).

HIGH-PERFORMANCE P&O-CPG ALGORITHM

According to the above, two main tasks exist - minimizing the overshoots and minimizing the power losses during the fast changing irradiance condition which has to be addressed in the case of CPG operation. The proposed high-performance P&O-CPG algorithm can effectively solve those issues.

A. Minimizing Overshoots Increasing the perturbation step size is a possibility to minimize the overshoots as the tracking speed is increased. Specifically, a large step size can reduce the required number of iterations to reach the corresponding CPP. Notably, the step size modification should be enabled only when the algorithm detects a fast increase in the Irradiance Condition (IC), which can be illustrated as

$$IC = \begin{cases} 1, & \text{when } P_{pv,n} - P_{limit} > \epsilon_{inc} \\ 0, & \text{when } P_{pv,n} - P_{limit} \leq \epsilon_{inc} \end{cases} \quad (3)$$

with P_{pv} being the measured PV power at the present sampling, and ϵ_{inc} being the criterion, which should be larger than the steady-state power oscillation of the PV panels. When a fast increase in the IC is detected (i.e., IC = 1), an adaptive step size is then employed, where the step size is calculated based on the difference between P_{limit} and $P_{pv,n}$ as it is given in (4). By doing so, the large step size will be used initially and the step size will continuously be reduced as the operating point approaches to the CPP.

$$v^*_{PV} = v_{pv,n} - \left[(P_{pv,n} - P_{limit}) \frac{P_{limit}}{P_{mp,y}} \right] \cdot v_{step} \quad (4)$$

where v_{pv} is the reference output voltage of the PV arrays, $v_{pv,n}$ and $P_{pv,n}$ are the measured output voltage and power of the PV array at the present sampling, respectively. P_{mp} is the rated power. v_{step} is the original step size of the P&O-CPG algorithm. The term $P_{limit}=P_{mp}$ is introduced to alleviate the step size dependency in the level of

P_{limit} . is a constant which can be used to tune the speed of the algorithm.

Minimizing Power Losses

As explained in Fig 7. when the CPG operating point is at the left side of the MPP, the P&O-CPG algorithm requires a number of iterations to reach the new MPP during a fast decrease in irradiance, leading to power losses. In fact, the operating point of the PV system does not change much if the PV system is operating in the MPPT under different irradiance levels as shown in Fig. 8. Notably, the detection of the decreased IC as well as the Previous Operating Mode (POM) is also important for minimizing the power losses:

$$IC = \begin{cases} 1, & \text{when } P_{PV,n-1} - P_{pv,n} > \epsilon_{dec} \\ 0, & \text{when } P_{PV,n-1} - P_{pv,n} \leq \epsilon_{dec} \end{cases} \quad (5)$$

$$POM = \begin{cases} CPG, & \text{when } |P_{limit} - P_{PV,n-1}| > \epsilon_{ss} \\ MPPT, & \text{when } |P_{limit} - P_{PV,n-1}| \leq \epsilon_{ss} \end{cases} \quad (6)$$

where "dec" and "ss" are criteria to determine the fast irradiance decrease and the CPG operating mode, respectively. $P_{pv,n-1}$ is the measured PV power at the previous sampling. For example, the value of "ss" can be chosen as 1-2 % of the rated power of the PV system, which is normally higher than the steady-state error in the PV power of the P&O-CPG algorithm. When a fast decrease (i.e., $IC = 1$) is detected during the CPG to MPPT transition according to (6), a constant voltage given by (7) is applied to the PV system in order to accelerate the tracking speed (i.e., minimize the power losses). The constant voltage can be approximated as 71-78 % of the open circuit voltage V_{OC} , as illustrated in Fig. 7.

$$v_{pv}^* = k \cdot V_{OC}, \text{ where } 0.71 \leq k < 0.78 \quad (7)$$

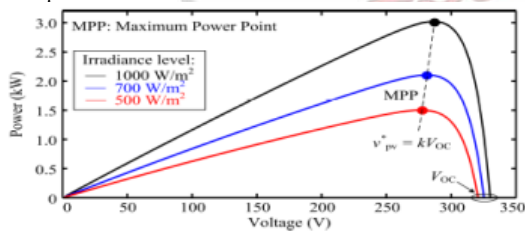


Fig. 7. Power-voltage (P-V) curves of the PV arrays, where the voltage at the MPP is almost constant especially at a higher irradiance level .

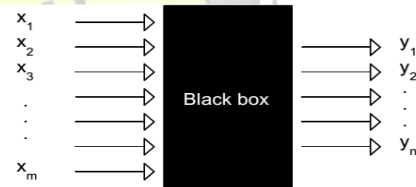
By doing so, the operating point can be instantaneously moved close to the MPP in one perturbation, resulting in a significant reduction in the number of iterations until the operating point reaches the MPP. This approach is simple but effective, which is very suitable to be implemented.

ARTIFICIAL NEURAL NETWORK

Introduction

In the last few decades, as the chemists have get accustomed to the use of computers and consequently to the implementation of different complex statistical methods. With the increasing accuracy and precision of analytical measuring methods it become clear that all effects that are of interest cannot be described by simple uni-variate and even not by the linear multivariate correlations precise, a set of methods, that have recently found very intensive use among chemists are the artificial neural networks (or ANNs for short).

Therefore, the analytical chemists are always eager to try all new methods that are available to solve such problems. One of the methods, or to say more Due to the fact that this is not one, but several different methods featuring a wide variety of different architectures learning strategies and applications.



Input variables Non-linear relation Output variables
Fig 8. Neural network as a black-box featuring the non-linear relationship between the multivariate input variables and multi-variate responses

BASIC CONCEPTS OF ANNS

Artificial neuron is supposed to mimic the action of a biological neuron, i.e., to accept many different signals, x_i , from many neighbouring neurons and to process them in a pre-defined simple way. Depending on the outcome of this processing, the neuron j decides either to fire an output signal y_j or not. The output signal (if it is triggered) can be either 0 or 1, or can have any real value between 0 and 1 (Fig. 2) depending on whether we are dealing with 'binary' or with 'real valued' artificial neurons, respectively.

The first function is a linear combination of the input variables, $x_1, x_2, \dots, x_i, \dots, x_m$, multiplied with the coefficients, w_{ji} , called 'weights', while the second function serves as a 'transfer function' because it 'transfers' the signal(s) through the neuron's axon to the other neurons' dendrites. Here, we shall show now how the output, y_j , on the j -th neuron is calculated. First, the net input is calculated according to equation

$$Net_j = \sum_{i=1}^m w_{ji}x_i \quad (7)$$

$$y_j = out_j = \frac{1}{\{1 + exp[-\alpha_j(Net_j + \theta_j)]\}} \quad (8)$$

The weights w_{ji} in the artificial neurons are the analogues to the real neural synapse strengths between the axons firing the signals.

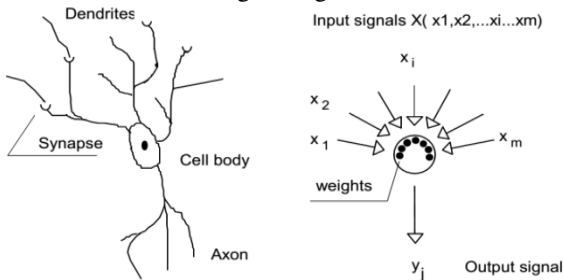


Figure 9. Comparison between the biological and artificial neuron. The circle mimicking the neuron's cell body represents simple mathematical procedure that makes one output signal y_j from the set input signals represented by the multi-variate vector X .

It is important to understand that the form of the transfer function, once it is chosen, is used for all neurons in the network, regardless of where they are placed or how they are connected with other neurons. What changes during the learning or training is not the function, but the weights and the function parameters that control the position of the threshold value, q_j , and the slope of the transfer function

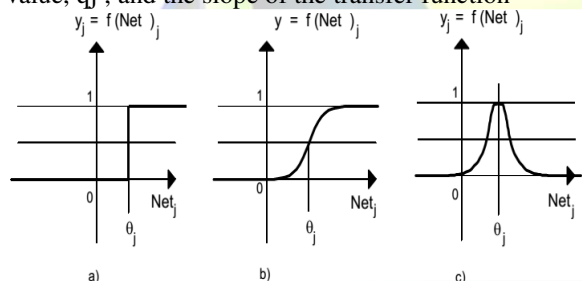


Figure 10. Three different transfer functions: a) threshold (a), a sigmoidal (b) and a radial function (c). The parameter q_j in all three functions decides the Net_j value around which the neuron is most selective.

Therefore, Figure shows actually a 2-layer and a 3-layer networks with the input layer being inactive. The reader should be careful when reading the literature on ANNs because authors sometimes actually refer to the above ANNs as to the two and three-layer ones. We shall regard only the active layer of neurons as actual layer and will therefore name this networks as one and two-layer ANNs.

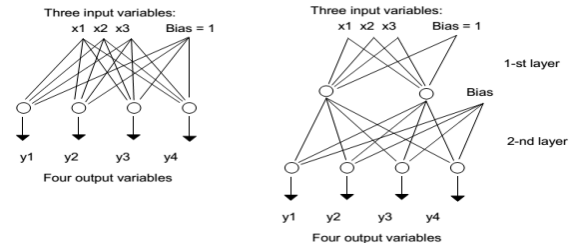


Figure 11. One-layer (left) and two-layer (right) ANNs. The ANNs shown can be applied to solve a 3-variable input 4-responses output problem

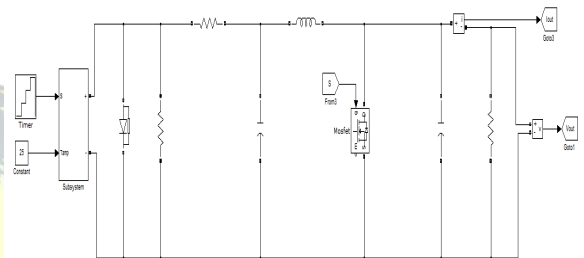


Fig.12. Block diagram of simulation

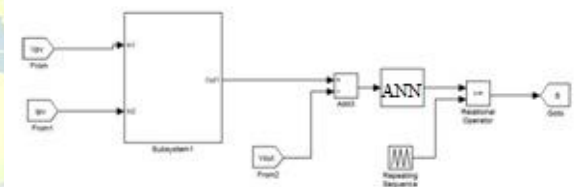


Fig.13. Control block diagram of simulation

SIMULATION VERIFICATION

Solutions to improve the dynamic performance of the P&OCPG algorithm have been discussed above. Parameters of the proposed high-performance P&O-CPG algorithm are designed as: $\alpha = 10$, $k = 0.715$, "inc = 50 W", "dec = 100 W", and "ss = 30 W". Simulation are carried out referring to Fig. 3, and the system parameters are given in Table II.

Table II
Parameters Of The Two-Stage Single-Phase Pv System

Boost converter inductor	$L = 1.8 \text{ mH}$
PV-side capacitor	$C_{pv} = 1000 \mu\text{F}$
DC-link capacitor	$C_{dc} = 1100 \mu\text{F}$
LCL-filter	$L_{inv} = 4.8 \text{ mH}$, $L_g = 4 \text{ mH}$, $C_f = 4.3 \mu\text{F}$
Switching frequency	Boost converter: $f_b = 16 \text{ kHz}$, Full-Bridge inverter: $f_{inv} = 8 \text{ kHz}$
DC-link voltage	$V_{dc} = 450 \text{ V}$
Grid nominal voltage (RMS)	$V_g = 230 \text{ V}$
Grid nominal frequency	$\omega_g = 2\pi \times 50 \text{ rad/s}$

In the simulation, a 3-kW PV simulator has been adopted, where real-field solar irradiance and ambient temperature profiles are programmed. Fig. shows the performance of the proposed high performance P&O-CPG method with two real-field

daily conditions. In contrast to the conventional P&O-CPG method (shown in Fig. 6), the overshoots and power losses are significantly reduced by the proposed solution and a stable operation is also maintained. The algorithm also has a selective behavior to only react, when the fast irradiance condition is detected. This can be seen from the performance under clear irradiance conditions in Fig. 14(a), which is similar to the conventional P&O-CPG algorithm (shown in Fig. 6(a)).

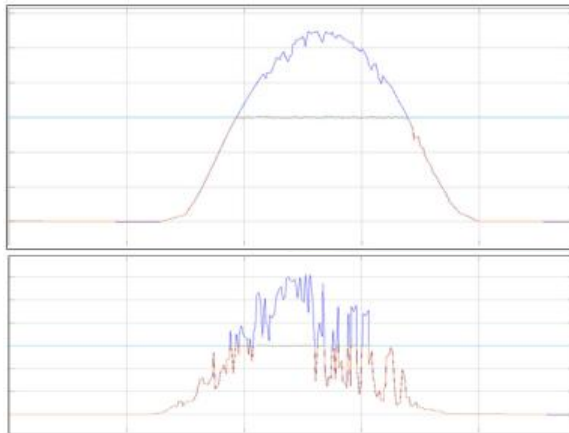


Fig. 14. simulation results of the proposed high-performance P&O-CPG algorithm under two daily conditions: (a) clear day and (b) cloudy day.

CONCLUSION

In this paper observed that an high-performance active power control scheme been limiting the maximum power which is feed to the PV systems which is proposed there. The proposed solution make sure about the stable constant power generation operation. When compared with the traditional methods. Here the proposed control strategy will forces the PV systems to operate at the left side of the maximum power point, and which make to achieve a stable operation along with smooth transitions. Neural networks offer a number of advantages, including requiring less formal statistical training, ability to implicitly detect complex nonlinear relationships between dependent and independent variables, ability to detect all possible interactions between predictor variables, and the availability of multiple training algorithms along with another controller because of the better performance. In ANN is non-paramateric model while most of statistical methods are parametric model that need higher background of statistic basic control action and improve the efficiency. Simulation have verified the effectiveness of the proposed control solution in order to minimized power losses, reduced overshoots

and also fast dynamics. Moreover for single-stage PV systems, same concept of CPG is also applicable. Therefore in such case, the PV voltage operating range will limited and some small changes in the algorithms which are necessary to make sure for a stable operation.

REFERENCES

- [1] T. Stetz, F. Marten, and M. Braun, "Improved low voltage gridintegration of photovoltaic systems in Germany," *IEEE Trans. Sustain. Energy*, vol. 4, no. 2, pp. 534–542, Apr. 2013.
- [2] A. Ahmed, L. Ran, S. Moon, and J.-H. Park, "A fast PV power tracking control algorithm with reduced power mode," *IEEE Trans. Energy Conversion*, vol. 28, no. 3, pp. 565–575, Sept. 2013.
- [3] Y. Yang, H. Wang, F. Blaabjerg, and T. Kerekes, "A hybrid power control concept for PV inverters with reduced thermal loading," *IEEE Trans. Power Electron.*, vol. 29, no. 12, pp. 6271–6275, Dec. 2014.
- [4] Christo Ananth, W. Stalin Jacob, P. Jenifer Darling Rosita. "A Brief Outline On ELECTRONIC DEVICES & CIRCUITS.", ACES Publishers, Tirunelveli, India, ISBN: 978-81-910-747-7-2, Volume 3, April 2016, pp:1-300.
- [5] Energinet.dk, "Technical regulation 3.2.5 for wind power plants with a power output greater than 11 kw," *Tech. Rep.*, 2010.
- [6] Y. Yang, F. Blaabjerg, and H. Wang, "Constant power generation of photovoltaic systems considering the distributed grid capacity," in *Proc. of APEC*, pp. 379–385, Mar. 2014.
- [7] I. Mr.S.Esakki Rajavel, Mr.B.Pradheep T Rajan and E.Edinda Christy, "Energy Efficient Collaborative Spectrum Sensing In Cognitive Radio Networks" *Global Research and Development Journal for Engineering(GRDJE)* ,Vol. 2, Issue 1, December 2016,Page No:26-29,ISSN (online) : 2455-5703
- [8] W. Cao, Y. Ma, J. Wang, L. Yang, J. Wang, F. Wang, and L. M. Tolbert, "Two-stage PV inverter system emulator in converter based power grid emulation system," in *Proc. of ECCE*, pp. 4518–4525, Sept. 2013.
- [9] A. Urtasun, P. Sanchis, and L. Marroyo, "Limiting the power generated by a photovoltaic system," in *Proc. of SSD*, pp. 1–6, Mar. 2013.
- [10] S. B. Kjaer, J. K. Pedersen, and F. Blaabjerg, "A review of single-phase grid-connected inverters for photovoltaic modules," *IEEE Trans. Ind. Appl.*, vol. 41, no. 5, pp. 1292–1306, Sept. 2005.
- [11] F. Blaabjerg, R. Teodorescu, M. Liserre, and A. V. Timbus, "Overview of control and grid synchronization for distributed power generation



systems,” IEEE Trans. Ind. Electron., vol. 53, no. 5, pp. 1398–1409, Oct. 2006.

[12] B. Yang, W. Li, Y. Zhao, and X. He, “Design and analysis of a gridconnected photovoltaic power system,” IEEE Trans. Power Electron., vol. 25, no. 4, pp. 992–1000, Apr. 2010.



D.ARAVIND

Completed B.Tech in Electrical & Electronics Engineering from St. Martin’s Engineering College and M.Tech in Power Electronics from CMR Engineering College and Technology, Hyderabad.

Working as Assistant Professor in St. Martin’s Engineering College, Dhullapally, Secunderabad, Telangana. Area of interest includes Power Electronics, FACTS Devices and Renewable Energy Sources.

E-mail id: aravind.smec204@gmail.com



V.SUNIL KUMAR

Completed B.Tech in Electrical & Electronics Engineering from Syed Hashim College of Science and Technology affiliated to JNTU Hyderabad

and M.Tech in Electrical Power Systems from B.S.A.Crescent Engineering College affiliated to Anna University, Chennai. He is working as Associate Professor in St. Martin’s Engineering College, Dhullapally, Secunderabad, Telangana. His Area of interest includes Power Systems, FACTS Devices and Renewable Energy Sources.

E-mail id: vskumar20@gmail.com.



ISMAYEL GOLLAPUDI

Received B.Tech degree from St. Ann’s college of Engineering and Technology (JNTUK) in the year 2009 and received M.Tech in the stream of Power

Electronics at SRI VASAVI ENGINEERING COLLEGE (JNTUK) in the year 2012. Currently working as a Assistant Professor in Malla Reddy Engineering College and Management sciences for Three years and totally i have 5 years experience in the teaching field. His areas of interest are Applications of Power electronics in “Control Systems, Power systems Electrical machines”.

Email id: gismayel214@gmail.com.